α-Helix targeting reduces amyloid-β peptide toxicity

C. Nerelius[a,1], A. Sandegren[a,1], H. Sargsyan[b], R. Raunak[b], H. Leijonmarck[b], U. Chatterjee[a], A. Fisahn[c], S. Imarisio[d], D. A. Lomas[e,f], D. C. Crowther[d,e], R. Strömberg[b,2], and J. Johansson[a,2]

[a]Department of Anatomy, Physiology and Biochemistry, Swedish University of Agricultural Sciences, The Biomedical Centre, S-751 23 Uppsala, Sweden; [b]Department of Biosciences and Nutrition at Novum, Karolinska Institutet, S-14157 Huddinge, Sweden; [c]Department of Neuroscience, Karolinska Institutet, S-17177 Stockholm, Sweden; Departments of [d]Genetics and [e]Medicine, University of Cambridge, Cambridge CB2 3EH, United Kingdom; and [f]Cambridge Institute for Medical Research, Cambridge CB2 0XY, United Kingdom

Edited by Jan-Ake Gustafsson, Karolinska Institutet, Stockholm, Sweden, and approved March 31, 2009 (received for review October 15, 2008)

The amyloid-β peptide (Aβ) can generate cytotoxic oligomers, and their accumulation is thought to underlie the neuropathologic changes found in Alzheimer's disease. Known inhibitors of Aβ polymerization bind to undefined structures and can work as nonspecific aggregators, and inhibitors that target conformations that also occur in larger Aβ assemblies may even increase oligomer-derived toxicity. Here we report on an alternative approach whereby ligands are designed to bind and stabilize the 13–26 region of Aβ in an α-helical conformation, inspired by the postulated Aβ native structure. This is achieved with 2 different classes of compounds that also reduce Aβ toxicity to cells in culture and to hippocampal slice preparations, and that do not show any nonspecific aggregatory properties. In addition, when these inhibitors are administered to *Drosophila melanogaster* expressing human Aβ_{1-42} in the central nervous system, a prolonged lifespan, increased locomotor activity, and reduced neurodegeneration is observed. We conclude that stabilization of the central Aβ α-helix counteracts polymerization into toxic assemblies and provides a strategy for development of specific inhibitors of Aβ polymerization.

amyloid fibrils | neurodegenerative disease | protein misfolding | Alzheimer's disease

Alzheimer's disease is a progressive neurodegenerative disorder that is characterized by cerebral extracellular amyloid plaques and intracellular neurofibrillary tangles (1). Classically, the amyloid cascade hypothesis (2) states that Alzheimer's disease is caused by fibril and plaque formation of amyloid-β peptide (Aβ) in the central nervous system. More recently, the hypothesis has been modified to include Aβ assemblies of sizes intermediate to monomeric and fibrillar forms, which today are considered to be the main source of cytotoxicity (3). Such Aβ assemblies include low-number oligomers and larger assemblies known as protofibrils, globulomers, Alzheimer's disease diffusible ligands, or Aβ*56 (4–7). Aβ is cleaved from an integral membrane protein, the amyloid β precursor protein (AβPP), predominantly as a 40-residue peptide (Aβ_{1-40}). In addition, a C-terminally elongated 42-residue version can be excised (Aβ_{1-42}); it is this longer variant that is the main constituent of parenchymal amyloid deposits (8).

The link between Aβ aggregation and Alzheimer's disease implies that inhibitors of this process should be able to slow down disease progression. A number of low-molecular-mass Aβ aggregation inhibitors have been identified by use of screens of compound libraries as well as rational design strategies. The resulting inhibitors include such chemically diverse compounds as curcumin, inositol, and nicotine (9, 10). The screens have identified inhibitors of fibril formation that similarly to the rationally designed inhibitors are predicted to bind to Aβ in an elongated, β-strand-like conformation and prevent its polymerization. A potential problem with this strategy is that blocking the later stages of fibril formation will favor the formation of prefibrillar oligomeric forms that are cytotoxic (10, 11). No Aβ oligomer has been structurally determined, and thus these oligomers cannot yet be targeted by rational design. A further problem with some of the Aβ polymerization inhibitors is that they can act as aggregators (12). Chemical aggregators can physically sequester proteins in a promiscuous and nonspecific manner and thereby interfere with fibril formation (13, 14). Such compounds are typically conjugated aromatics, hydrophobic and dye-like (12), features that are common among published inhibitors of Aβ aggregation. In light of these circumstances, alternative strategies to reduce Aβ aggregation and toxicity are warranted. One possible approach, explored herein, is to trap Aβ in a state similar to its perceived structure in membrane-embedded AβPP, by targeting the central discordant α-helix region.

Aβ_{1-40} and Aβ_{1-42} are mainly disordered in water but deviate from a completely random coil by the presence of local, nonrandom conformations (15). Trends toward nonrandom structures for the peptide segments 8–12, 16–24, and 30–34 of both Aβ_{1-40} and Aβ_{1-42} were identified by NMR. Residues 20–24 form a helical turn, and the segment 16–24 shows several hydrophobic contacts between side-chains. Although Aβ_{1-40} and Aβ_{1-42} show different aggregation behavior, whereby the latter is much more prone to aggregate, their solution structures were found to be practically identical, but Aβ_{1-42} is more rigid in the C-terminal region (15, 16). Moreover, Aβ_{1-42} shows β-strand structure in the regions 31–36 and 39–41, whereas Aβ_{1-40} lacks tendency for β-strand structure in the 29–40 region (17). In the presence of detergent micelles or structure-inducing organic solvents, both Aβ_{1-40} and Aβ_{1-42} adopt more stable secondary structural elements (18). The structures determined in such environments differ slightly from each other, but collectively they show that the regions covering residues 15–24 and 29 to the C terminus form α-helices. In SDS micelles the Aβ_{1-40} helix covering residues 15–24 is located on the surface with residues 16, 20, 22, and 23 oriented toward the surrounding solvent, whereas another helix covering residues 29–35 (which are part of the AβPP transmembrane region) is buried in the hydrophobic interior of the micelle (19). We show here that compounds designed to interact with and stabilize the Aβ_{13-23} helix alter the aggregation properties of Aβ in vitro and reduce Aβ toxicity toward PC12 cells and hippocampal slice preparations. Moreover, the administration of these compounds in fly food reduces the toxicity of the Aβ_{1-42} peptide in a *Drosophila melanogaster* model of Alzheimer's disease.

Author contributions: C.N., A.S., A.F., R.S., and J.J. designed research; C.N., A.S., H.S., R.R., H.L., U.C., A.F., S.I., and D.C.C. performed research; D.A.L. and D.C.C. contributed new reagents/analytic tools; C.N., A.S., A.F., S.I., D.C.C., R.S., and J.J. analyzed data; and C.N., A.S., R.S., and J.J. wrote the paper.

Conflict of interest statement: J.J. and R.S. have research grants and stock options from AlphaBeta AB, a company that aims to use the strategy described for treatment of Alzheimer's disease.

This article is a PNAS Direct Submission.

[1]C.N. and A.S. contributed equally to this article.

[2]To whom correspondence may be addressed. E-mail: roger.stromberg@ki.se or jan.johansson@afb.slu.se.

This article contains supporting information online at www.pnas.org/cgi/content/full/0810364106/DCSupplemental.

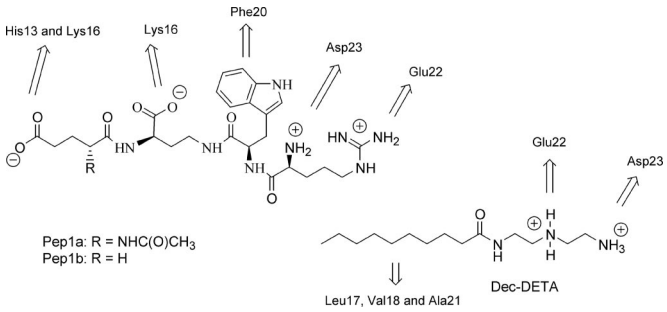

Fig. 1. Ligands designed for binding to the α-helical form of the 13–23 region of the Aβ peptide. Arrows indicate the amino acids in Aβ with which the different groups are designed to interact.

Results

Design of Inhibitors. The amino acid sequence of Aβ_{16-23} has a strong statistical preference for β-strand structure, constituting a so-called discordant α-helix (20), and forms a β-strand in Aβ fibrils (21, 22). The α-helical form of this region of the Aβ-peptide provides a suitable target for stabilizing ligands. Residues 13–26 of human Aβ (Aβ_{13-26}; H^{13}HQKLVFFAEDVGS^{26}), including the discordant region, were built into an α-helical conformation using molecular graphics. For possible interaction we concentrated on 2 partial surfaces of this helix. One side of the helix is largely hydrophobic and adjacent to Glu-22 and Asp-23. A hydrocarbon chain could potentially interact with this surface. Also adjacent to Glu-22 and Asp-23 is a surface containing Phe-20, which connects these residues with Lys-16 and His-13. To investigate the concept we evaluated possible chemical interactions by building molecular structures that could be initial potential ligands for these surfaces. The hydrophobic region is adjacent to 2 carboxylate functions, and therefore it seemed obvious to combine a hydrophobic tail with a cationic function. This interaction was tested with a readily made molecule, N^1-decanoyl-diethylenetriamine (Dec-DETA; Fig. 1). The surface connecting the Asp-23 and Glu-22 with Lys-16 and His-13 was targeted by the peptoid structure Pep1a, which was later simplified to Pep1b (Fig. 1). The Pep1 structures were built for potential interaction with Asp-23 and Glu-22 via the 2 positive charges on the arginine moiety and with Lys-16 and a partially protonated His-13 via the carboxylate groups. Additional hydrophobic interaction with Phe-20 was devised through the D-Trp residue. The built complexes between the peptide and the potential ligands were also submitted to short sessions of molecular dynamics simulations at 310 K. Starting with Aβ_{13-26} in α-helical conformation, Aβ alone starts to unfold and lose its helical structure during the simulation, whereas in the presence of either ligand the helical conformation remains (Fig. 2).

Effects on Aβ Secondary Structure and Aggregation. Circular dichroism (CD) spectroscopy showed that addition of ligands affected the secondary structure of Aβ_{12-28} (Fig. 3). For all 3 ligands an increase in negative ellipticity around 222 nm, indicative of increased helical content, was observed. However, the spectra in the presence of ligands are not typical for peptides with only helical secondary structure. This is likely to result from spectral contributions from populations of partially aggregated Aβ_{12-28} or from the residues outside the 13–23 region. We therefore synthesized a more stable peptide that covered the target region (Aβ residues 13–23) with 4 alanines on either side (Aβ_{13-23A}). Addition of the ligands to this peptide showed a clear increase in helical content, with higher amplitudes at 190, 208, and 222 nm [supporting information (SI) Fig. S1]. Under conditions whereby the Aβ peptides are structurally disordered as assessed by their CD spectra, no or very small effects on the secondary structure could be observed (data not shown), in keeping with the ligand design to target α-helical Aβ. Finally, the ligand-induced effects are Aβ sequence dependent, given that a variant of the alanine-containing peptide in which the sequence of Aβ_{13-23} was scrambled was unaffected in the presence of ligands (Fig. S2). These data show that the ligands Pep1 and Dec-DETA bind to and stabilize Aβ species that populate helical conformations in the region 13–23.

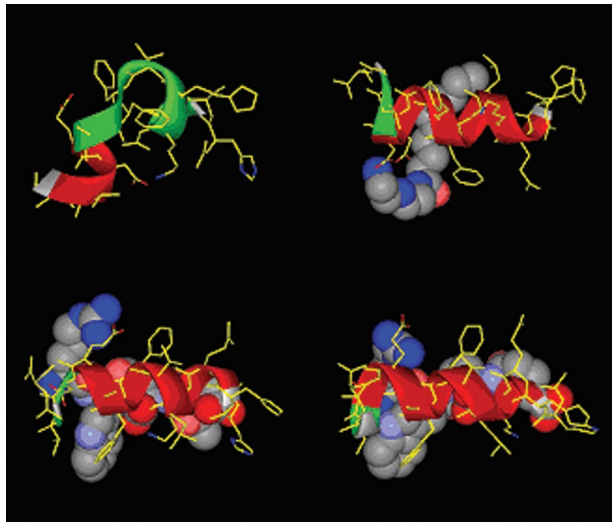

Fig. 2. Molecular modeling of stabilization of α-helical Aβ by ligands. Representations of the conformation of the Aβ_{13-26} peptide after a brief molecular dynamics run (using the Discover engine, Amber force field, and a dielectric continuum environment) in the absence (*Top Left*) of ligand and in the presence of Dec-DETA (*Top Right*), Pep1a (*Bottom Left*), or Pep1b (*Bottom Right*). Ligands rendered as Corey–Pauling–Koltun (CPK) representations and Aβ_{13-26} as stick models with overlayed ribbon (colored red where the secondary structure type is α-helical).

The effects of Pep1 and Dec-DETA on Aβ fibril formation

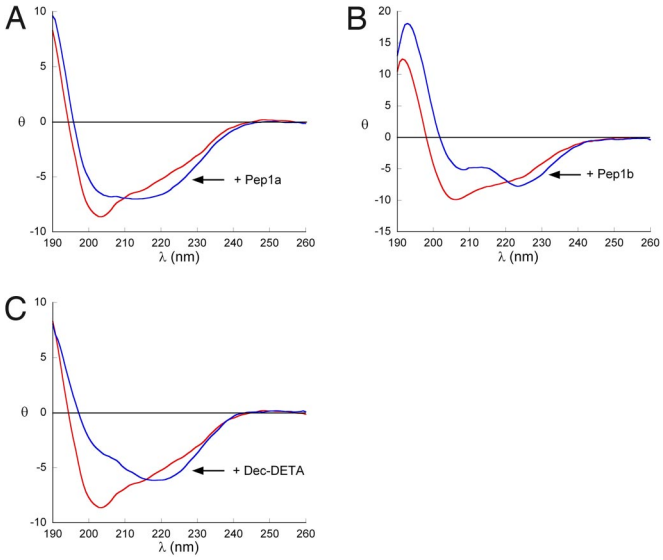

Fig. 3. Ligand effects on secondary structure of Aβ_{12-28}. Far-UV circular dichroism spectra recorded in 10 mM phosphate buffer (pH 7) containing 20% vol/vol trifluoroethanol of Aβ_{12-28} alone (red lines) or with (blue lines) ligands Pep1a (*A*) in a 1:1 molar ratio, Pep1b (*B*) in a 1:1 molar ratio, and Dec-DETA (*C*) in a 1:5 molar ratio. Mean molar residual ellipticity is expressed as kdeg $\times$ cm^2/dmol.

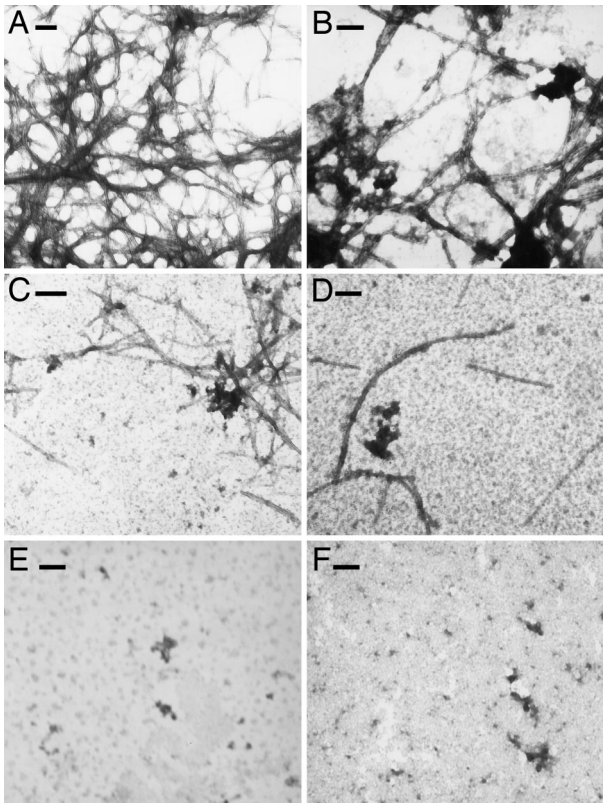

Fig. 4. Ligands affect fibril formation of $A\beta_{1-40}$. Transmission electron microscopy show fibrils formed from (*A*) 25 μM $A\beta_{1-40}$ incubated alone or with addition of 25 μM of (*B*) Pep1a, (*C*) Pep1b, or (*D*) Dec-DETA. The bottom row shows incubated samples containing (*E*) 125 μM Pep1b and (*F*) 125 μM Dec-DETA alone. All incubations were done at 37 °C with agitation. (Scale bars, 100 nm.)

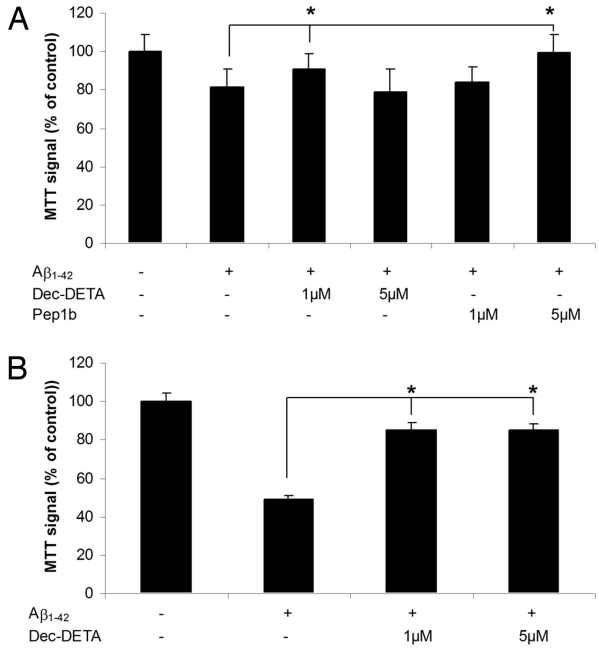

Fig. 5. Reduction of $A\beta_{1-42}$ toxicity to PC12 cells. (*A*) PC12 cells were treated with $A\beta_{1-42}$ (1 μM) alone or with Pep1b (1 and 5 μM) or Dec-DETA (1 and 5 μM) for 4 h, after which cellular metabolic capacities were assayed by MTT reduction. (*B*) MTT signal of PC12 cells treated either with $A\beta_{1-42}$ (1 μM) alone or with Dec-DETA (1 and 5 μM) for 18 h. Control treatment is set to 100%. Error bars represent SEM ($n = 3$). *$P < 0.05$, as analyzed by Student's *t* test. One representative experiment out of 3 is shown.

were investigated with the fluorescent dye thioflavin T, which binds to β-sheets, and electron microscopy. Incubation of $A\beta_{1-40}$ with Pep1a or Pep1b reduces the amount of fibrils detectable by electron microscopy. With Pep1b hardly any fibrils were detected, and the ones found were shorter than ordinary Aβ fibrils (Fig. 4 and Fig. S3). In agreement with this, Pep1 prolongs the lag-phase before thioflavin T fluorescence of $A\beta_{1-40}$ polymers starts to increase and also reduces thioflavin T fluorescence of $A\beta_{1-40}$ at later time points (Fig. S3). Dec-DETA gave reduced amounts of Aβ fibrils by electron microscopy (Fig. 4), whereas $A\beta_{1-40}$ incubated with Dec-DETA showed larger increase in thioflavin T fluorescence compared with $A\beta_{1-40}$ alone (Fig. S3). The reason for this is unclear but may be related to the appearance of fibrils shorter and thicker than the typical Aβ fibrils (Fig. S3).

Ligands Reduce Aβ Toxicity In Vitro and In Vivo. Aβ polymerization generates assemblies that are toxic to cells in culture. MTT [3-(4, 5-dimethylthiazol-2-yl)-2–5 diphenyltetrazolium bromide] was used to monitor oxidative capacity of PC12 cells after treatment with $A\beta_{1-42}$ polymerized in the presence of the different ligands. Dec-DETA and Pep1b reduced the toxic effects of $A\beta_{1-42}$ (Fig. 5*A*). In addition, Dec-DETA reduced the more pronounced Aβ toxicity produced by longer incubation times (Fig. 5*B*). Pep1b effects on $A\beta_{1-42}$ during longer incubation times could not be evaluated because Pep1b alone was toxic to the PC12 cells under these conditions (approximately 90% MTT signal compared with controls).

To study whether the ligands could influence a more relevant physiologic activity in the context of Alzheimer's disease, we tested their effect on pharmacologically induced rhythmic network activity in the γ-frequency range [20–80 Hz, γ oscillations (23, 24)] in hippocampal slice preparations. Gamma oscillations play an important role in higher processes in the brain, such as learning, memory, cognition, and perception (25), and are markedly reduced in patients diagnosed with Alzheimer's disease (26) or schizophrenia (27, 28). Incubation of slices in artificial cerebrospinal fluid (ACSF) containing $A\beta_{1-42}$ before induction of γ oscillations significantly reduced the average oscillation power compared with naïve slices incubated in ACSF alone (Fig. 6*B*). This Aβ-induced reduction in oscillation power was strongly attenuated when Pep1b and Dec-DETA, respectively, were added to the incubation solution (Fig. 6 *A* and *C*). Incubation with ligands alone did not significantly affect oscillation power compared with naïve conditions (Fig. 6*C*).

Transgenic *Drosophila melanogaster* expressing the human $A\beta_{1-42}$ gene in the neurones of the central nervous system provide a model system for studying the consequences of $A\beta_{1-42}$ aggregation in vivo. The Aβ-expressing flies exhibit a markedly reduced survival compared with wild-type flies (29). Congo Red, a compound known to reduce the aggregation of Aβ, reduces toxicity in this *Drosophila* model of disease (29). To evaluate the effect of Dec-DETA and Pep1a on the longevity of transgenic $A\beta_{1-42}$ *Drosophila*, the flies were continually exposed to the compounds from the embryonic stage onward and throughout adult life. Treatment with 3.1 mM as well as 31 μM Dec-DETA prolonged the median lifespan of the flies from 9 to 12 days (Fig. 7). Pep1a showed a rescue of survival at 200 μM and a trend toward prolonging lifespan at 2 μM (median survival for both concentrations, 12 days; Fig. 7). Dec-DETA and Pep1a had no effect on the lifespan of nontransgenic w^{1118} wild-type flies (Fig. 7), thereby indicating that the compounds' mode of action is Aβ dependent. In addition, the effect of Dec-DETA and Pep1a was assessed in the transgenic fly model at 28 °C rather than 29 °C,

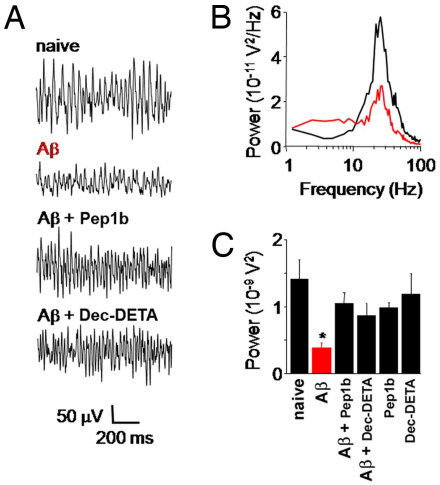

Fig. 6. Ligands reverse Aβ-induced reduction of γ oscillation power in hippocampal slices. (*A*) In response to 100 nM kainate all slices generated γ oscillations in area CA3. Incubation in 1 μM $A\beta_{1-42}$ (4 h) before kainate superfusion significantly reduced γ oscillation power ($P = 0.006$). Addition of 5 μM of either Pep1b or Dec-DETA to the 1-μM Aβ incubation solution reversed the decrease in oscillation power. (*B*) Power spectra of γ oscillations in a naïve slice and after incubation with Aβ. (*C*) Summary histogram of γ oscillation power in naïve slices ($1.41 \pm 0.29\ 10^{-9}V^2$; $n = 10$), $A\beta_{1-42}$ incubated slices ($0.37 \pm 0.09\ 10^{-9}V^2$; $n = 10$), $A\beta_{1-42}$+Pep1b incubated slices ($1.05 \pm 0.16\ 10^{-9}V^2$; $n = 8$), $A\beta_{1-42}$+Dec-DETA incubated slices ($0.87 \pm 0.18\ 10^{-9}V^2$; $n = 8$), Pep1b-only incubated slices ($0.98 \pm 0.07\ 10^{-9}V^2$; $n = 8$), and Dec-DETA-only incubated slices ($1.18 \pm 0.31\ 10^{-9}V^2$; $n = 8$).

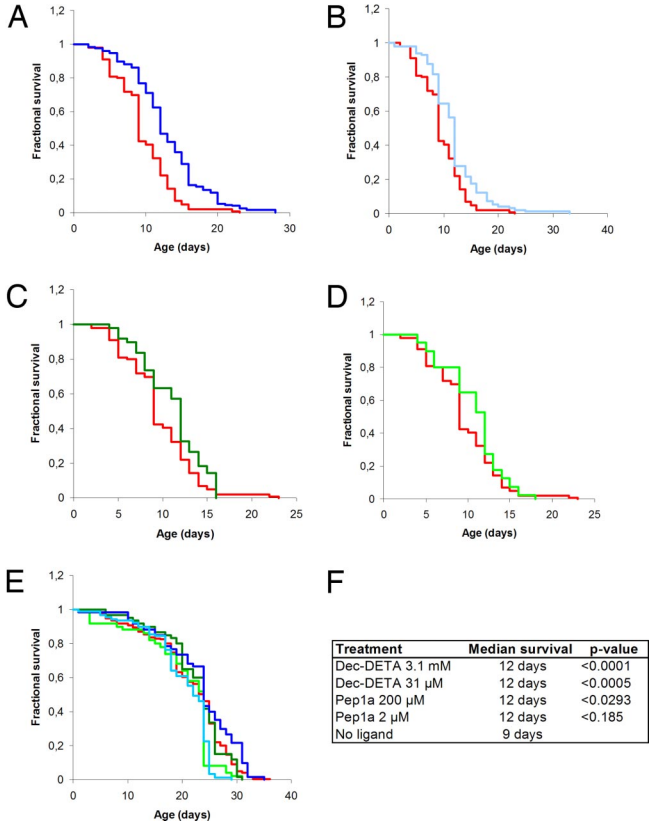

Fig. 7. Ligands prolong lifespan of $A\beta_{1-42}$ transgenic flies. Longevity analysis of *Drosophila melanogaster* at 29 °C. (*A–D*) Kaplan-Maier survival plots of nontreated $A\beta_{1-42}$ flies (red; $n = 99$) and $A\beta_{1-42}$ flies treated with (*A*) 3.1 mM Dec-DETA (dark blue; $n = 128$), (*B*) 31 μM Dec-DETA (light blue; $n = 98$), (*C*) 200 μM Pep1a (dark green; $n = 49$), and (*D*) 2 μM Pep1a (light green; $n = 40$). (*E*) Kaplan-Maier survival plots of nontreated w^{1118} flies ($n = 168$) and w^{1118} flies treated with Dec-DETA [3.1 mM ($n = 50$) and 31 μM ($n = 60$)] and with Pep1a [200 μM ($n = 60$) and 2 μM ($n = 89$)], color coding as in *A–D*. (*F*) List of median survival and *P* values compared with nontreated $A\beta_{1-42}$ flies for Kaplan-Maier curves presented in *A–D*.

which results in a slightly weaker phenotype. The compounds improved the survival of Aβ-expressing flies at the lower temperature, and once again wild-type w^{1118} were not affected by the treatment (Fig. S4). Finally, no significant rescue of neurotoxicity, measured as the number of surviving photoreceptor cells, after treatment with 2 or 200 μM Pep1b was seen using constitutive expression of mutant huntingtin in the *Drosophila* eye (Fig. S5), again pointing to the specificity whereby the ligand seems to exert its effect.

Drosophila flies expressing $A\beta_{1-42}$ show progressive loss of locomotor activity, eventually resulting in almost complete immobility (29). A clear improvement in mobility was observed in the Aβ-expressing flies that were fed Dec-DETA. In a climbing assay performed on 16-day-old flies kept at 28 °C, 6 of 9 treated flies reached the upper half of the tube during a 0.5-min observation, whereas 1 of 10 of the control-treated flies climbed the same distance (Movie S1).

In histologic examinations of sectioned fly heads a difference in tissue appearance was observed between Dec-DETA–treated and control Aβ-expressing flies (Fig. 8). In nontreated Aβ transgenic flies the progressive nervous tissue degradation from post-eclosion day 0 to day 10 was significantly more pronounced than in Dec-DETA–treated flies (Table 1), showing a high degree of destroyed nervous tissue in the eye and part of the brain. Wild-type w^{1118} flies did not exhibit any change in tissue condition for the same time period (data not shown), suggesting that the tissue destruction was Aβ related and that treatment with Dec-DETA had a rescuing effect on this process.

The abilities of Dec-DETA and Pep1b to aggregate and to nonspecifically affect enzyme activity were assessed. Neither Dec-DETA nor Pep1b gives rise to any aggregates detectable by electron microscopy (Fig. 4), none of the compounds has any inhibitory effect on alcohol dehydrogenase activity (Table S1), and Dec-DETA has a critical micelle concentration >2 mM. These data indicate that none of the compounds acts as an aggregator. Thus, the observed effects of Dec-DETA and Pep1 on Aβ are concluded to be specific, in contrast to some of the previously described inhibitors of Aβ polymerization (12).

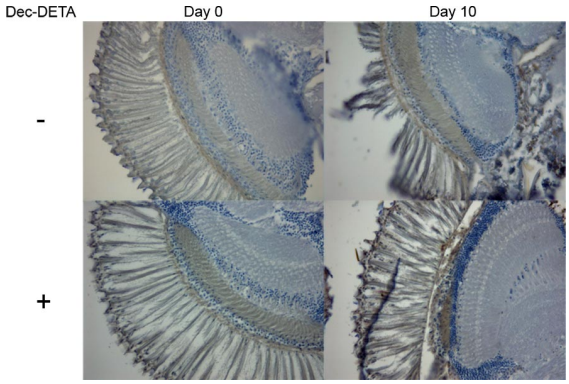

Fig. 8. Dec-DETA affects nervous tissue destruction in transgenic flies. Histology of brain and eye from $A\beta_{1-42}$ transgenic flies at day 0 or day 10 after eclosion. The flies were either nontreated controls or treated with 4.9 mM Dec-DETA. Ten-micrometer sections of flyheads were immunostained using the anti-Aβ monoclonal antibody 4G8, and the integrity of the nerve tissue in the eye and brain was assessed in a blinded setup. The images are representative of a set with $n = 6–11$ flies (see Table 1).

Table 1. Integrity of brain and eye tissue of flies expressing two copies of the Aβ_{1-42} transgene

Group	n	Score, median (range)
Non-treated day 0	11	2(1–3)
Non-treated day 10	6	4(1–5)*
Dec-DETAday 0	9	1(1–3)
Dec-DETA day 10	11	2(1–4)

The flies were either control or treated with 4.9 mM Dec-DETA. Tissue destruction was assessed based on the appearance of the nervous tissue in the eye and brain of the immunostained sections. Tissue destruction scores; 1: intact nervous tissue, 2: <25% of the nervous tissue destroyed, 3: 25–50% destroyed, 4: 51–75% destroyed, 5: 76–100% destroyed. The identities of the samples were blinded to the examiner. * $P < 0.05$ vs non-treated at day 0. There was a trend towards statistical significance between flies treated with ligand and non-treated at day 10 ($P = 0.07$).

Discussion

Pep1 and Dec-DETA affect Aβ helical content, polymerization, and toxicity in vitro and in vivo. These molecules represent 2 different classes of compounds, which supports that the effects observed on Aβ aggregation and toxicity are caused by interactions expected from their design rather than from nonspecific binding events.

The in vivo effects of Pep1a and Dec-DETA observed in a *Drosophila* model of Aβ aggregation are encouraging because they indicate that both compounds, after administration in the fly food, target Aβ expressed in the central nervous system of a whole organism. The locomotor and climbing phenotypes of the *Drosophila* model closely reflect the aggregation propensities of Aβ variants (30). It should be emphasized that in the flies, Aβ is expressed at elevated levels, without its precursor, and only short-term effects are monitored. When Aβ is excised from AβPP in humans its environment changes, and the regions that are α-helical are expected to lose their helical structure. A molecule that stabilizes, even modestly, the α-helical structure should cause a delay of the subsequent β-sheet oligomerization and aggregation.

No disease-modifying drug for Alzheimer's disease is available, and clinical trials of potential drugs have so far been discouraging. However, several compounds that affect Aβ polymerization have been identified using different approaches (see, e.g., refs. 31–37). These compounds lack structurally defined targets, and some of them may work in a nonspecific manner. The present investigation suggests that targeting the central α-helix of monomeric Aβ, the structure of which is defined at atomic resolution, offers a novel approach to finding specific inhibitors of Aβ aggregation that are effective in vivo.

Materials and Methods

Synthesis of Ligands. Synthesis of Dec-DETA was carried out by condensation of decanoic acid with diethylenetriamine in the presence of isobutyl chloroformate. The Pep1 structures were synthesized using activated pentafluorophenyl esters and appropriately protected and/or activated building blocks of D-Trp, L-Arg, D-diaminobutanoic acid, and D-Glu or glutaric acid (Schemes S1 and S2).

CD Spectroscopy. Twenty-five micromolar of Aβ_{12-28} or the different variants of Aβ_{13-23} were mixed with 25 μM ligand in 10 mM sodium phosphate buffer (pH 7) with 0, 20%, or 25% (vol/vol) trifluoroethanol. CD spectra were obtained using aJasco J-810–150S spectropolarimeter. A quartz cell with 1-mm optical path was used. Spectra were recorded at 22 °C between 185 and 260 nm with a bandwidth of 1 nm, a 2-s response time, and a scan speed of 50 nm/min. Background spectra, and when applicable, spectra of Pep1 or Dec-DETA were subtracted and the results expressed as mean molar residual ellipticity. Each spectrum represents the average of 3 consecutive scans.

Transmission Electron Microscopy. Twenty-five micromolar of Aβ_{1-40} was incubated with or without ligand (0, 25, or 125 μM) for time periods spanning from 24 h up to 7 days at 37 °C under agitation. At each time point aliquots of 2 μL were adsorbed for 1 min on 200-mesh copper grids. The grids were then stained with 2% uranyl acetate for 30 s and examined and photographed using a Hitachi H7100 microscope operated at 75 kV.

Cell Culture Experiments. PC12 cells were cultured in 5% CO_2 in DMEM supplemented with 10% FCS and penicillin/streptomycin (National Veterinary Institute, Sweden). The cells were plated at an appropriate density in 96-well Cell+ plates (Sarstedt). The following day the media were exchanged to DMEM without phenol red (45 μL/well) supplemented with 10% FCS and penicillin/streptomycin. Aβ_{1-42} at 10 μM was added (5 μL/well), resulting in a final concentration of 1 μM either directly (4-h treatment experiment) or after 4 h preincubation at 37 °C (18-h treatment experiment), alone or with Dec-DETA or Pep1b at equimolar or 5× molar excess concentration. PBS with the same amount of solvent used for the Aβ preparations was used as control treatment. The cells were incubated for 4 or 18 h with treatment, and thereafter MTT dissolved at 0.6 mg/mL in DMEM without phenol red was added (50 μL/well), resulting in a final concentration of 0.3 mg/mL MTT, and incubated with the cells for 2 h at 37 °C. The purple formazan crystals were dissolved using a solubilization buffer containing 50% dimethylformamide and 20% SDS in water added directly to the cell culture media (100 μL/well). Absorbance at 575 nm was recorded and control treatment set to 100%. Results were statistically analyzed by Student's *t* test.

Electrophysiology. Horizontal hippocampal slices (400 μm) from 14-week-old C57/Bl6 wild-type mice were maintained at 22 °C in a submerged holding chamber containing ACSF (in mM: NaCl 124, KCl 3.5, NaH_2PO_4 1.25, $MgCl_2$ 1.5, $CaCl_2$ 1.5, $NaHCO_3$ 30, and glucose 10) and aerated with 95% O_2/5% CO_2. The holding chamber also contained either 1 μM Aβ_{1-42}, 5 μM of either Pep1b or Dec-DETA, or combinations thereof. All slices were incubated for 4 h before recording. Extracellular recordings were made in stratum pyramidale of area CA3 in an interface recording chamber (30 °C) using glass microelectrodes containing ACSF (resistance, 3–5 MΩ). Kainate (100 nM) was used to induce γ oscillations (Tocris). Data were recorded with an extracellular field amplifier (Cologne University, Germany) using pClamp 9.2 software (Molecular Devices). Fast Fourier transformations for power spectra were computed from 60-s-long data traces using Axograph software (Molecular Devices). Gamma oscillation power values were obtained by integrating power spectra over the γ-frequency band (20–80 Hz) (i.e., measuring the area underneath the spectral graph between 20 and 80 Hz). Data values are given as mean ± SEM. Student's *t* test was used for statistics.

Transgenic Flies and Longevity Assay. Aβ transgenic *Drosophila melanogaster* strains were generated as described by Crowther et al. (29). Transgenic flies expressing 2 gene copies of human Aβ_{1-42}, 1 on chromosome 2 and 1 on chromosome 3, were obtained by crossing Aβ flies with flies transgenic for the Gal4-*elav*^{c155} pan-neuronal driver.

Flies expressing Aβ_{1-42} were incubated in groups of 10 in 10-cm glass vials. Wild-type w^{1118} flies treated the same way as the Aβ flies were used as controls. The flies were kept either at 29 °C and high humidity or at 28 °C and low humidity. Larvae were fed instant fly food containing either 3.1 mM or 31 μM Dec-DETA (at 29 °C) or 4.9 mM Dec-DETA (at 28 °C), and Pep1a was administered at 200 μM or 2 μM (at 29 °C) or at 0.65 mM (at 28 °C) until eclosion. Thereafter flies were fed standard fly food with a streak of yeast paste containing the same amount as stated above of Dec-DETA and Pep1a, respectively. Food was changed every second day, and viable flies were counted. Survival data were analyzed using the WinStat Kaplan-Meier software package (R. Fitch Software). Longevity of the flies depends substantially on conditions such as humidity and temperature and therefore varies between experimental occasions. For that reason, treated and non-treated control Aβ-expressing flies and wild-type w^{1118} flies were kept in the same incubator (i.e., under identical conditions).

Histologic Examination. To evaluate degree of tissue destruction, immunostained sections of fly brains and eyes were scored according to a 5-point scale, where 1 indicates intact tissue and 5 indicates >75% destroyed tissue. The specimens were blinded to the examiner. Histologic scores were statistically analyzed by one-way ANOVA, nonparametric as described by Kruskal-Wallis, followed by Dunn's multiple comparison posttest. The data were evaluated using GraphPad Prism 4.02 software.

Detailed descriptions are available in *SI Materials and Methods*.

ACKNOWLEDGMENTS. We thank Drs. Gilad Silberberg and Per Westermark for help with electrophysiology and histology experiments. S.I. was supported by Drs. C. J. O'Kane and D. C. Rubinsztein and funded by United Kingdom Medical Research Council Grant G0600194. D.C.C. was supported by United Kingdom Medical Research Council Grant G0700990. This work was supported by the Swedish Research Council and the Swedish Brain Foundation.

1. Selkoe DJ (1991) The molecular pathology of Alzheimer's disease. *Neuron* 6:487–498.
2. Hardy J, Higgins GA (1992) Alzheimer's disease: The amyloid cascade hypothesis. *Science* 256:184–185.
3. Hardy J, Selkoe DJ (2002) The amyloid hypothesis of Alzheimer's disease: Progress and problems on the road to therapeutics. *Science* 297:353–356.
4. Hartley DM, et al. (1999) Protofibrillar intermediates of amyloid β-protein induce acute electrophysiological changes and progressive neurotoxicity in cortical neurons. *J Neurosci* 19:8876–8884.
5. Lambert MP, et al. (1998) Diffusible, nonfibrillar ligands derived from Aβ1–42 are potent central nervous system neurotoxins. *Proc Natl Acad Sci USA* 95:6448–6453.
6. Lesne S, et al. (2006) A specific amyloid-β protein assembly in the brain impairs memory. *Nature* 440:352–357.
7. Walsh DM, et al. (2002) Naturally secreted oligomers of amyloid β protein potently inhibit hippocampal long-term potentiation in vivo. *Nature* 416:535–539.
8. Iwatsubo T, et al. (1994) Visualization of Aβ 42(43) and Aβ 40 in senile plaques with end-specific Aβ monoclonals: Evidence that an initially deposited species is Aβ 42(43) *Neuron* 13:45–53.
9. Mason JM, Kokkoni N, Stott K, Doig J (2003) Design strategies for anti-amyloid agents. *Curr Opin Struct Biol* 13:526–532.
10. LeVine, III, H (2007) Small molecule inhibitors of Aβ assembly. *Amyloid* 14:185–197.
11. Cohen FE, Kelly JW (2003) Therapeutic approaches to protein-misfolding diseases. *Nature* 426:905–909.
12. Feng BY, et al. (2008) Small-molecule aggregates inhibit amyloid polymerization. *Nat Chem Biol* 4:197–199.
13. McGovern SL, Caselli E, Grigorieff N, Shoichet K (2002) A common mechanism underlying promiscuous inhibitors from virtual and high-throughput screening. *J Med Chem* 45:1712–1722.
14. McGovern SL, Helfand BT, Feng B, Shoichet K (2003) A specific mechanism of nonspecific inhibition. *J Med Chem* 46:4265–4272.
15. Riek R, Güntert P, Döbeli H, Wipf B, Wüthrich K (2001) NMR studies in aqueous solution fail to identify significant conformational differences between the monomeric forms of two Alzheimer peptides with widely different plaque-competence, Aβ(1–40)(ox) and Aβ(1–42)(ox). *Eur J Biochem* 268:5930–5936.
16. Yan Y, Wang C (2006) Aβ42 is more rigid than Aβ40 at the C terminus: Implications for Aβ aggregation and toxicity. *J Mol Biol* 364:853–862.
17. Hou L, et al. (2004) Solution NMR studies of the Aβ(1–40) and Aβ(1–42) peptides establish that the Met35 oxidation state affects the mechanism of amyloid formation. *J Am Chem Soc* 126:1992–2005.
18. Serpell LC (2000) Alzheimer's amyloid fibrils: Structure and assembly. *Biochim Biophys Acta* 1502:16–30.
19. Jarvet J, Danielsson J, Damberg P, Oleszczuk M, Gräslund A (2007) Positioning of the Alzheimer Aβ(1–40) peptide in SDS micelles using NMR and paramagnetic probes. *J Biomol NMR* 39:63–72.
20. Kallberg Y, Gustafsson M, Persson B, Thyberg J, Johansson J (2001) Prediction of amyloid fibril-forming proteins. *J Biol Chem* 276:12945–12950.
21. Luhrs T, et al. (2005) 3D structure of Alzheimer's amyloid-β(1–42) fibrils. *Proc Natl Acad Sci USA* 102:17342–17347.
22. Petkova AT, et al. (2002) A structural model for Alzheimer's β-amyloid fibrils based on experimental constraints from solid state NMR. *Proc Natl Acad Sci USA* 99:16742–16747.
23. Fisahn A (2005) Kainate receptors and rhythmic activity in neuronal networks: Hippocampal gamma oscillations as a tool. *J Physiol* 562:65–72.
24. Fisahn A, Pike FG, Buhl EH, Paulsen O (1998) Cholinergic induction of network oscillations at 40 Hz in the hippocampus in vitro. *Nature* 394:186–189.
25. Engel AK, Singer W (2001) Temporal binding and the neural correlates of sensory awareness. *Trends Cogn Sci* 5:16–25.
26. Ribary U, et al. (1991) Magnetic field tomography of coherent thalamocortical 40-Hz oscillations in humans. *Proc Natl Acad Sci USA* 88:11037–11041.
27. Spencer KM, et al. (2004) Neural synchrony indexes disordered perception and cognition in schizophrenia. *Proc Natl Acad Sci USA* 101:17288–17293.
28. Wilson TW, et al. (2008) Cortical γ generators suggest abnormal auditory circuitry in early-onset psychosis. *Cereb Cortex* 18:371–378.
29. Crowther DC, et al. (2005) Intraneuronal Aβ, non-amyloid aggregates and neurodegeneration in a *Drosophila* model of Alzheimer's disease. *Neuroscience* 132:123–135.
30. Luheshi LM, et al. (2007) Systematic in vivo analysis of the intrinsic determinants of amyloid-β pathogenicity. *PLoS Biol* 5:e290.
31. Gervais F, et al. (2007) Targeting soluble Aβ peptide with Tramiprosate for the treatment of brain amyloidosis. *Neurobiol Aging* 28:537–547.
32. McLaurin J, et al. (2006) Cyclohexanehexol inhibitors of Aβ aggregation prevent and reverse Alzheimer phenotype in a mouse model. *Nat Med* 12:801–808.
33. Nakagami Y, et al. (2002) A novel β-sheet breaker, RS-0406, reverses amyloid β-induced cytotoxicity and impairment of long-term potentiation in vitro. *Br J Pharmacol* 137:676–682.
34. Necula M, Kayed R, Milton S, Glabe G (2007) Small molecule inhibitors of aggregation indicate that amyloid β oligomerization and fibrillization pathways are independent and distinct. *J Biol Chem* 282:10311–10324.
35. Soto C, et al. (1998) β-sheet breaker peptides inhibit fibrillogenesis in a rat brain model of amyloidosis: Implications for Alzheimer's therapy. *Nat Med* 4:822–826.
36. Townsend M, et al. (2006) Orally available compound prevents deficits in memory caused by the Alzheimer amyloid-β oligomers. *Ann Neurol* 60:668–676.
37. Yang F, et al. (2005) Curcumin inhibits formation of amyloid β oligomers and fibrils, binds plaques, and reduces amyloid in vivo. *J Biol Chem* 280:5892–5901.